Structural Engineering and Mechanics, *Vol. 76, No. 1 (2020) 101-114*
DOI: https://doi.org/10.12989/sem.2020.76.1.101

Nonlinear identification of Bouc–Wen hysteretic parameters using improved experience-based learning algorithm

Weili Luo[1], Tongyi Zheng[1], Huawei Tong*[1], Yun Zhou[1] and Zhongrong Lu[2]

[1]*School of Civil Engineering, Guangzhou University, Guangzhou, P.R. China*
[2]*Department of Applied Mechanics, Sun Yat-sen University, Guangzhou, P.R. China*

(Received February 12, 2020, Revised May 7, 2020, Accepted May 18, 2020)

Abstract. In this paper, an improved experience-based learning algorithm (EBL), termed as IEBL, is proposed to solve the nonlinear hysteretic parameter identification problem with Bouc-Wen model. A quasi-opposition-based learning mechanism and new updating equations are introduced to improve both the exploration and exploitation abilities of the algorithm. Numerical studies on a single-degree-of-freedom system without/with viscous damping are conducted to investigate the efficiency and robustness of the proposed algorithm. A laboratory test of seven lead-filled steel tube dampers is presented and their hysteretic parameters are also successfully identified with normalized mean square error values less than 2.97%. Both numerical and laboratory results confirm that, in comparison with EBL, CMFOA, SSA, and Jaya, the IEBL is superior in nonlinear hysteretic parameter identification in terms of convergence and accuracy even under measurement noise.

Keywords: experience-based learning; Bouc–Wen model; hysteretic parameters; nonlinear system identification; lead-filled steel tube dampers

1. Introduction

The nonlinear hysteretic effect has been found in many physical systems such as structural dampers, mechanical systems with joints, base-isolation devices for buildings, and piezoelectric materials (Tran and Li 2018, Li and Shu 2019, Korayem and Sadeghzadeh 2009, Korayem *et al.* 20012, Korayem and Homayouni 2017). One of the mathematical models, the Bouc-Wen model, has been extensively employed in describing the nonlinear hysteretic of civil and mechanical systems due to its numerical tractability and capability in capturing hysteresis loop in an analytical form (Shu and Li 2017, Dong *et al.* 2019). However, it is a challenging task to accurately estimate parameters of the Bouc–Wen model due to its highly nonlinear and memory nature.

Many researchers formulated the parameter identification problem of the Bouc–Wen model as a discrete state identification problem. For instance, Chang and Shi (2010) introduced a wavelet multiresolution technique for identifying time-varying parameters of hysteretic structures. Omrani *et al.* (2012) conducted the parameter identification of the Bouc-Wen model through an unscented Kalman filtering approach. More recently, Bajrić and Høgsberg (2018) proposed an output-only system identification method for estimating model parameters of a dynamic system with hysteretic damping. Niola *et al.* (2019) presented a constrained unscented Kalman filter for identifying hysteresis model parameters of the Bouc-Wen model that was adopted to describe the hysteretic shear behavior of a seismic isolator. However, this kind of identification method is generally complicated and often requires a high sampling rate because the discrete state equations should be accurate enough to approximate the original time-varying differential equations.

Alternatively, techniques based on metaheuristic stochastic algorithms attract growing interests for solving such nonlinear optimization problems in recent years. For example, Worden and Manson (2012) proposed a self-adaptive differential evolution algorithm for identifying nonlinear parameters of dynamical systems. Ortiz (*et al.* 2013) employed a multi-objective evolutionary optimization algorithm for identifying the parameters of the Bouc–Wen–Baber–Noori model. Quaranta *et al.* (2014) adopted PSO and DE for solving the parameter identification problem of Bouc–Wen model. Ding *et al.* (2019) proposed an improved tree-seed algorithm for determining parameters of nonlinear hysteretic systems. In most of these studies, stiffness and viscous damping of the Bouc-Wen model are usually given. This is not realistic for practical engineering problems, all parameters (including hysteretic parameter, stiffness, and viscous damping) need to be identified simultaneously.

Recently, a novel heuristic algorithm named experience-based learning algorithm (EBL) has been proposed for dealing with structural damage identification problems by the authors' team (Zheng *et al.* 2019). The attractive features of this algorithm are its simple principle, fast convergence, and algorithm-specific parameter-free characteristics, which are beneficial for achieving excellent performance in searching global optimal solutions. Nevertheless, like other heuristic algorithms, the EBL may inevitably suffer from the imbalance between the

*Corresponding author, Professor
E-mail: hwt@gzhu.edu.cn; 108211132@qq.com

http://www.techno-press.com/journals/sem&subpage=7 ISSN: 1225-4568 (Print), 1598-6217 (Online)

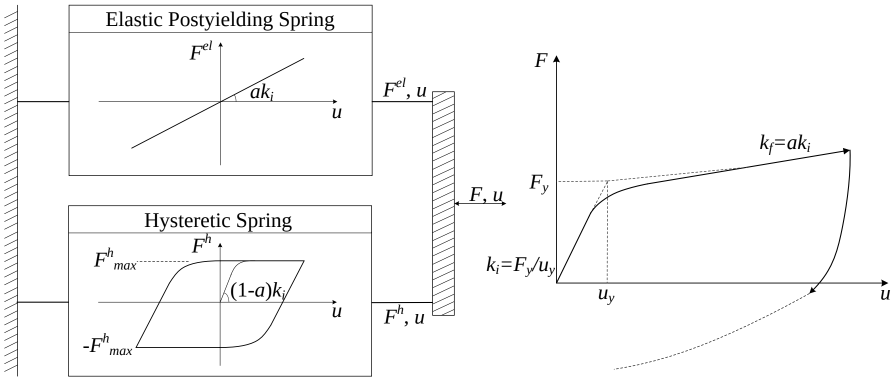

Fig. 1 Definiton of Bouc–Wen model.

exploration and exploitation capabilities. Therefore, it is important to well-balance the exploration and exploitation abilities in order to obtain better convergence performance and more precise results.

In this paper, an improved experience-based learning algorithm, namely IEBL, is proposed for Bouc–Wen hysteretic parameter identification, in which two modifications are introduced, including a concept of opposition-based learning and new updating equations for candidates. The quasi-oppositional learning handles a wider exploration of the search space, and the new updating equations enhance the exploitation capability by making use of more candidate information. Numerical simulations on a single-degree-of-freedom (SDOF) system are carried out to demonstrate the effectiveness of the proposed algorithm in comparison to the EBL and other four state-of-the-art algorithms including cloud model based fruit fly optimization algorithm (CMFOA) (Zheng *et al.* 2018), squirrel search algorithm (SSA) (Jain *et al.* 2019), and Jaya (Artar and Daloglu 2019). The influences of measurement noise and excitation input are also investigated. At last, a laboratory test of lead-filled steel tube dampers is presented and their parameters are identified to demonstrate the potential of the proposed algorithm for practical application.

The rest of this paper is organized as follows. Section 2 describes the problem formulation for nonlinear hysteretic parameter identification of the Bouc-Wen model. Section 3 briefly recapitulates the original EBL and describes the proposed IEBL with two modifications. Section 4 shows the results of numerical simulations. Section 5 presents a laboratory test of seven lead-filled steel tube dampers and their identified hysteretic parameters. Finally, concluding remarks are drawn in Section 6.

2. Problem statement

2.1 Hysteresis Bouc-Wen model

The equation of motion of a SDOF system is expressed as:

$$m\ddot{u}(t) + c\dot{u}(t) + F(t) = f(t) \tag{1}$$

where m is the mass, $u(t)$ is the displacement, c is the linear viscous damping, $F(t)$ is the restoring force, and $f(t)$ is the excitation force. The memory-based relationship between the displacement $u(t)$ and the restoring force $F(t)$ is expressed as (Ding 2019):

$$F(t) = a\frac{F_y}{u_y}u(t) + (1-a)F_y z(t) \tag{2}$$

where a is the ratio of post-yield to pre-yield (elastic) stiffness, F_y is the yield force, u_y is the yield displacement, and $z(t)$ is a non-observable hysteretic displacement that obeys the following nonlinear differential equation with zero initial condition ($z(0) = 0$):

$$\dot{z}(t) = \frac{1}{u_y}\left[A - |z(t)|^n\left(\beta + sign\left(\dot{u}(t)z(t)\right)\gamma\right)\right]\dot{u}(t) \tag{3}$$

where $sign$ is the signum function, and n, A, β, and γ are dimensionless quantities that control the size and the shape of the hysteretic loop. Dimensionless quantity n determines the shape of the transition from elastic to post-elastic branch: the transition tends to be smooth if parameter n is small while the transition for a large value of n becomes abrupt. Dimensionless quantity A is usually set to unity, and a constraint $A/(\beta+\gamma) = 1$ ($\gamma \in [0,1]$) is also imposed in order to eliminate the inherent functionally redundant problem of the model (Ma *et al.* 2004). In this way, the total number of unknown parameters is reduced to six, i.e. u_y, F_y, a, γ, n and c. A vector $\widehat{\boldsymbol{\theta}}$ containing the model's unknown parameters is defined as:

$$\widehat{\boldsymbol{\theta}} = \{u_y, F_y, a, \gamma, n, c\} \tag{4}$$

The restoring force $F(t)$ can be divided into an elastic part and a hysteretic part as follows:

$$F^{el}(t) = a\frac{F_y}{u_y}u(t) \tag{5}$$

$$F^h(t) = (1-a)F_y z(t) \tag{6}$$

Therefore, as shown in Fig.1, the restoring force can be visualized as two springs connected in parallel with $k_i = F_y/u_y$ and $k_f = ak_i$ being defined as the initial and post-yielding stiffness of the system, respectively.

2.2 Objective function for optimization problem

Nonlinear system identification with hysteretic models can be formulated as an optimization problem. The objective function of the optimization problem is defined as a function of the unknown parameter vector $\hat{\boldsymbol{\theta}}$ which can later be identified by minimizing the objective function through a specified heuristic algorithm. In this study, the objective function is constructed from the measured time history response of the model $y(t)$ and the estimated time history response $\hat{y}(t)$. At the kth time step t_k, the estimated response $\hat{y}(t_k)$ is defined as follows

$$\hat{y}(t_k) = f(\hat{\boldsymbol{\theta}}, t_k) \tag{7}$$

where $\hat{y}(t_k)$ can be displacement, velocity, acceleration, or force response. The objective function is defined as the normalized mean square error (MSE) of the estimated time history $\hat{y}(t)$ as compared to the measured time history response $y(t)$ of the model:

$$obj(\hat{\boldsymbol{\theta}}) = \frac{\sum_{k=1}^{n_{time}} \left(y(t_k) - \hat{y}(t_k)\right)^2}{N\sigma_y^2} \tag{8}$$

where n_{time} is the number of time steps; σ_y^2 is the variance of the measured time history response. Hence, the identification problem can be summarized as the minimization of the objective function $obj(\hat{\boldsymbol{\theta}})$ when the parameter vector $\hat{\boldsymbol{\theta}}$ is subjected to the feasible parameter side constraints Γ:

$$\text{Find } \hat{\boldsymbol{\theta}} \in \Gamma \text{ such that } obj(\hat{\boldsymbol{\theta}}) \to min \tag{9}$$

$$\Gamma = \{\hat{\boldsymbol{\theta}} \in \mathbb{R}^d | \theta_j^{min} \le \hat{\theta}_j \le \theta_j^{max}, j = 1, 2, \dots, d\} \tag{10}$$

where d is the number of parameters to be identified; θ_j^{min} and θ_j^{max} are the lower and upper bounds of model parameters, respectively. The objective function generally has multiple local minima to which the traditional optimization techniques are easy to be stuck. This may lead to poor identification results. Therefore, it is necessary to develop a powerful algorithm in order to deal with the nonlinear identification problem.

3. Improved experience-based learning algorithm

3.1 Original EBL

The EBL was a recently proposed heuristic algorithm for structural damage identification problems, inspiring by a learning strategy following the experience of a randomly chosen candidate of the population (Zheng *et al.* 2019). The initial step of the EBL is to generate a random initial set of N candidates in the specified searching space, among which the candidate that yields the smallest objective function value in Eq. (8) is selected as the initial best population. The core of the EBL is the phase of updating the new position of each candidate in its vicinity according to the following two modes of learning strategy:

Mode 1:

$$\hat{\theta}_{ij}^{new} = \begin{cases} \hat{\theta}_{ij} + rand \cdot D \cdot (\hat{\theta}_{ij} - \hat{\theta}_{lj}), if\ obj(\hat{\theta}_{ij}) < obj(\hat{\theta}_{lj}) \\ \hat{\theta}_{ij} + rand \cdot D \cdot (\hat{\theta}_{lj} - \hat{\theta}_{ij}), \quad otherwise \end{cases} \tag{11}$$

$$D = 1 - \left(\frac{Iter}{Iter_{max}}\right) \cdot \exp\left(\frac{Iter}{Iter_{max}}\right) \tag{12}$$

Mode 2:

$$\hat{\theta}_{ij}^{new} = \begin{cases} \hat{\theta}_{ij} + rand \cdot (\hat{\theta}_{ij} - rand \cdot \hat{\theta}_{lj}), if\ obj(\hat{\theta}_{ij}) < obj(\hat{\theta}_{lj}) \\ \hat{\theta}_{ij} + rand \cdot (\hat{\theta}_{lj} - rand \cdot \hat{\theta}_{ij}), \quad otherwise \end{cases} \tag{13}$$

where $\hat{\theta}_{ij}^{new}$ indicates the jth component ($j = 1, 2, \dots, d$) of the new ith candidate ($i = 1, 2, \dots, N$); $\hat{\theta}_{ij}$ represents the jth component of the present ith candidate; $\hat{\theta}_{lj}$ is the jth component of a randomly selected lth candidate with $l \ne i$; $Iter_{max}$ is the maximum number of iteration; N is the number of population size; $rand$ is a uniformly distributed random number in the range [0, 1]. In Mode 1, a new candidate is produced by moving the old candidate towards the randomly chosen one in the population with an exploring radius dynamically changing with iteration. In Mode 2, a new candidate is generated in the vicinity of its old candidate based on the experience of the randomly chosen candidate $\hat{\theta}_{lj}$. In order to balance the exploration and exploitation abilities of the algorithm during the searching process, these two modes are called randomly in each iteration. To further enhance the intensive search of each dimension, a dimensional search strategy is carried out for the best-so-far candidate in a way that all dimensions of the candidate are updated independently:

$$\hat{\theta}_{best,j}^{new} = \hat{\theta}_{best,j} + rand \cdot (1 - \frac{Iter}{Iter_{max}})^{10} \cdot (\hat{\theta}_{best,j} - \hat{\theta}_{worst,j}), j = 1, 2, \dots, d \tag{14}$$

3.2 Improved EBL algorithm

Two modifications are introduced in the IEBL in order to improve the optimization performance of the EBL and to balance its exploration and exploitation abilities, including quasi-oppositional-based learning and new updating equations.

3.2.1 Modification 1: Quasi-oppositional-based learning

The concept of opposition-based learning is to simultaneously consider the current candidate and its opposite to find a solution efficiently, which is typically useful for escaping from local optima. This concept has been successfully applied in many soft computing algorithms for enhancing their optimization performance (Mahdavi *et al.* 2018). In the IEBL, population candidates and their opposite to the candidates are generated, and both are considered at the same time before the two modes of learning strategy. In order to maintain the stochastic nature of the IEBL, the quasi-opposite candidate $\hat{\theta}_{ij}^{q}$ of a candidate $\hat{\theta}_{ij}$ is introduced:

$$\hat{\theta}_{ij}^{q} = \begin{cases} cs + rand \cdot (mp - cs), \quad if\ mp > cs \\ mp + rand \cdot (cs - mp), otherwise \end{cases}, i = 1, 2, \dots, N \tag{15}$$

$$cs = \frac{\theta^{max} + \theta^{min}}{2} \tag{16}$$

$$mp = \theta^{max} + \theta^{min} - \hat{\theta}_{ij} \tag{17}$$

where *cs* is the center of search space, mp is the mirror of the candidate $\hat{\theta}_{ij}$. After the generation of *N* quasi-opposite candidates, the fitness values of the original *N* candidates and the *N* quasi-opposite candidates are calculated and ranked in a descending order, from which the first N candidates are selected for the present population. In this way, the candidates are able to explore a much larger region of the search space, thus enhancing the exploration ability of the algorithm.

3.2.2 Modification 2: New updating equations for solution search

In the original EBL, the phase of updating a new position of one candidate $\hat{\theta}_{ij}^{new}$ in its vicinity is conducted by either Eq. (11) or (13). It can be observed that the experience of only one individual candidate $\hat{\theta}_{lj}$ is employed. This does not make full use of information hidden in other candidates, especially the information of the current best candidate, and thus may lead to a premature convergence in the case with multiple local optima. To address this problem, new updating equations are introduced by utilizing the information of the current best candidate $\hat{\theta}_{best,j}$ and another three randomly chosen candidates $\hat{\theta}_{lj}$, $\hat{\theta}_{mj}$ and $\hat{\theta}_{nj}$. Hence, the two modes are modified as follows:

(1) *Mode 1*:

$$\hat{\theta}_{ij}^{new} = \begin{cases} \hat{\theta}_{ij} + rand \cdot D \cdot \left(\hat{\theta}_{best,j} - \hat{\theta}_{lj}\right), if\ obj\left(\hat{\theta}_{ij}\right) < obj\left(\hat{\theta}_{lj}\right) \\ \hat{\theta}_{nj} + rand \cdot D \cdot \left(\hat{\theta}_{mj} - \hat{\theta}_{lj}\right), \quad otherwisre \end{cases} \tag{18}$$

$$D = 1 - \left(\frac{Iter}{Iter_{max}}\right) \cdot \exp\left(\frac{Iter}{Iter_{max}}\right) \tag{19}$$

Mode 2:

$$\hat{\theta}_{ij}^{new} = \begin{cases} \hat{\theta}_{ij} + rand \cdot \left(\hat{\theta}_{best,j} - rand \cdot \hat{\theta}_{lj}\right), if\ obj\left(\hat{\theta}_{ij}\right) < obj\left(\hat{\theta}_{lj}\right) \\ \hat{\theta}_{nj} + rand \cdot \left(\hat{\theta}_{mj} - rand \cdot \hat{\theta}_{lj}\right), \quad otherwisre \end{cases} \tag{20}$$

In the original EBL, the two modes are called in a random manner. In order to further balance the search performance and to control the convergence rate, a nonlinear factor (NF) is introduced to dynamically adjust the use of two modes in each iteration:

$$NF = \left(1 - \frac{Iter}{Iter_{max}}\right)^{20} \tag{21}$$

If $NF < rand$, the new position of candidate $\hat{\theta}_{ij}^{new}$ is updated by Mode 1; otherwise, $\hat{\theta}_{ij}^{new}$ is updated by Mode 2.

A step-by-step pseudocode of the IEBL is presented in Algorithm 1.

Algorithm 1 Pseudocode of IEBL

Set $Iter_{max}$, N, d, θ^{min} and θ^{max}
Randomly initialize candidates
$\hat{\theta}_{ij} = \theta^{min} + rand * (\theta^{max} - \theta^{min}), i = 1, 2, \ldots, N, j = 1, 2, \ldots, d$
Calculate fitness value
$f_i = obj\left(\hat{\theta}_{i1}, \hat{\theta}_{i2}, \ldots, \hat{\theta}_{id}\right), i = 1, 2, \ldots, N$
while $Iter < Iter_{max}$
Generate quasi-opposite population
$cs = \frac{\theta^{max} + \theta^{min}}{2}$, $mp = \theta^{max} + \theta^{min} - \hat{\theta}_{ij}$
$\hat{\theta}_{ij}^{q} = \begin{cases} cs + rand \cdot (mp - cs), \ if\ mp > cs \\ mp + rand \cdot (cs - mp), otherwise \end{cases}, i = 1, 2, \ldots, N,$
Select good candidates from the original population and the quasi-opposite population
Update new position of population
for i=1: N
Calculate NF
$NF = \left(1 - \frac{Iter}{Iter_{max}}\right)^{20}$
Find $\hat{\theta}_{best,j}$ and randomly select $\hat{\theta}_{lj}$, $\hat{\theta}_{mj}$ and $\hat{\theta}_{nj}$
if $NF < rand$
$D = 1 - \left(\frac{Iter}{Iter_{max}}\right) \cdot exp\left(\frac{Iter}{Iter_{max}}\right)$
$\hat{\theta}_{ij}^{new} = \begin{cases} \hat{\theta}_{ij} + rand \cdot D \cdot \left(\hat{\theta}_{best,j} - \hat{\theta}_{lj}\right), if\ f\left(\hat{\theta}_{ij}\right) < f\left(\hat{\theta}_{lj}\right) \\ \hat{\theta}_{nj} + rand \cdot D \cdot \left(\hat{\theta}_{mj} - \hat{\theta}_{lj}\right), \quad otherwisre \end{cases}$
else
$\hat{\theta}_{ij}^{new} = \begin{cases} \hat{\theta}_{ij} + rand \cdot \left(\hat{\theta}_{best,j} - rand \cdot \hat{\theta}_{lj}\right), if\ f\left(\hat{\theta}_{ij}\right) < f\left(\hat{\theta}_{lj}\right) \\ \hat{\theta}_{nj} + rand \cdot \left(\hat{\theta}_{mj} - rand \cdot \hat{\theta}_{lj}\right), \quad otherwisre \end{cases}$
end
Calculate fitness value of new population
if $f\left(\hat{\theta}_{ij}^{new}\right) < f\left(\hat{\theta}_{ij}\right)$
$\hat{\theta}_{ij} = \hat{\theta}_{ij}^{new}$
end
end
Enhance intensive dimensional search
Find $\hat{\theta}_{best,j}, \hat{\theta}_{worst,j}, f_{best}$
for j=1 : d
$\hat{\theta}_{best,j}^{new} = \hat{\theta}_{best,j} + rand \cdot (1 - \frac{Iter}{Iter_{max}})^{10} \cdot \left(\hat{\theta}_{best,j} - \hat{\theta}_{worst,j}\right), j = 1, 2, \ldots, d$
Calculate fitness value of the new candidate
$f_{best}^{new} = f\left(\hat{\theta}_{best,1}, \hat{\theta}_{best,2}, \ldots, \hat{\theta}_{best,j}^{new}, \ldots, \hat{\theta}_{best,d}\right)$
if $f_{best}^{new} < f_{best}$
$\hat{\theta}_{best,j} = \hat{\theta}_{best,j}^{new}$
$f_{best} = f_{best}^{new}$
end
end
$Iter = Iter + 1$
end

Table 1 Identification case studies in the numerical studies

Case No.	Loading scenario*	Parameters	Algorithms	Noise level
1	d	$u_y,\ F_y,\ a,\ \gamma,\ n$	IEBL, EBL, CMFOA, SSA, Jaya	0%
2	a, b, c, d	$u_y,\ F_y,\ a,\ \gamma,\ n$	IEBL	0%
3	c	$u_y,\ F_y,\ a,\ \gamma,\ n$	IEBL, EBL, CMFOA, SSA, Jaya	10%
4	d	$u_y,\ F_y,\ a,\ \gamma,\ n,\ c$	IEBL, EBL, CMFOA, SSA, Jaya	0%
5	b, c, d	$u_y,\ F_y,\ a,\ \gamma,\ n,\ c$	IEBL, EBL	0%
6	d	$u_y,\ F_y,\ a,\ \gamma,\ n,\ c$	IEBL	0%, 5%, 10%

*Loading scenario a: $u = 0.5u_y \sin t$; b: $u = 2u_y \sin t$; c: $u = 7u_y \sin t$; d: $f(t) = 5/2\cos(t/2)$.

Table 2 Parameter settings for the involved algorithms.

Algorithm	Maximal iteration number	Population size	Other parameters
IEBL	500	25	-
EBL	500	50	-
CMFOA	500	50	$En_{\max} = (X_{\max} - X_{\min})/4$
SSA	500	50	$G_c = 1.9, sf = 18, P_{dp} = 0.01$
Jaya	500	50	-

Table 3 True values and constraints in the cases with no viscous damping

Parameters	u_y (m)	F_y (kN)	a (-)	γ (-)	n (-)	c (kNs/m)
True values	0.1	3	0.1	0.9	2	0
Lower bound	0	0	0	0	0	-
Upper bound	1	10	1	1	10	-

4. Numerical studies

In this section, a series of numerical simulations have been carried out for a SDOF system without/with viscous damping in order to investigate the effectiveness of the proposed IEBL for nonlinear identification of Bouc–Wen hysteretic parameters. Numerical results are compared with the other four state-of-the-art algorithms (the original EBL, CMFOA, SSA, and Jaya). A list of six case studies is summarized in Table 1.

4.1 Parameter setting for the algorithms

The maximal iteration number and the population size are set to the same values for EBL, CMFOA, SSA, and Jaya, which are 500 and 50, respectively. The population size of IEBL is a half of that of the other algorithms and equals 25 because the first modification of IEBL doubles the population number at the beginning of each iteration. The same set of the initial random population is used for all algorithms. Ten independent runs are carried out in each case study to obtain meaningful statistic results. Table 2 lists the parameter settings of all algorithms.

4.2 Parameter identification without viscous damping

Three case studies are carried out in this section with four scenarios of input excitation. Three (Scenarios a-c) are displacement-controlled sinusoidal inputs with amplitudes being 0.5, 2.0, and 7.0 times the yield displacement, respectively; one (Scenario d) is force-controlled input with an external loading $f(t) = 5/2\cos(t/2)$ and a mass $m = 25$. The initial displacement, velocity, and restoring force of the system are all set to be zero. The time history of acceleration is used to construct the objective function. The total time is 6π with a sampling rate of 50 Hz. Table 3 shows the true parameter values and the lower and upper bound constraints. Fig. 2 shows the true hysteretic loops under the four input excitations.

4.2.1 Case 1: Identification of Scenario d without noise

This case study aims to test the effectiveness of IEBL on the identification of hysteretic parameters of Bouc-Wen nonlinear model without viscous damping. Table 4 shows the final identification results with the mean detected values and the corresponding relative errors. It is found that IEBL is able to accurately identify the hysteretic parameters of the Bouc-Wen model without any estimation errors. However, EBL, CMFOA, SSA, and Jaya cannot identify the hysteretic parameters exactly with maximum errors of 0.10%, 39.65%, 2.10%, and 0.02%, respectively. Fig. 3 shows the average evolutionary process of the fitness values for all five algorithms in a logarithmic form. It can be observed that the fitness values of IEBL converge more quickly than those of the EBL, CMFOA, SSA, and Jaya, indicating that the identified results of proposed IEBL are the closest to the true parameter values. The final identified results obtained by the IEBL are much more reliable with the best precision. For instance, Fig. 4 shows a comparison between the true hysteresis loop and the loop calculated by IEBL and CMFOA. In Fig. 4(a), a perfect match is observed between the curve identified by IEBL and the true one. By contrast, the curve identified by CMFOA does not fit the true one very well, as presented in Fig. 4(b). This comparison confirms the superiority of the IEBL in identifying the Bouc-Wen hysteretic parameters.

4.2.2 Case 2: Influence of excitation input

This case study is to test the influence of excitation input. Four types of input are investigated. For a fair comparison, only the IBEL is used in the present case study. Table 5 lists the statistical results in terms of the mean value and relative error. It can be found that in Scenario a the relative errors of the IEBL are rather large. This is because the response in the scenario is almost linear and does not

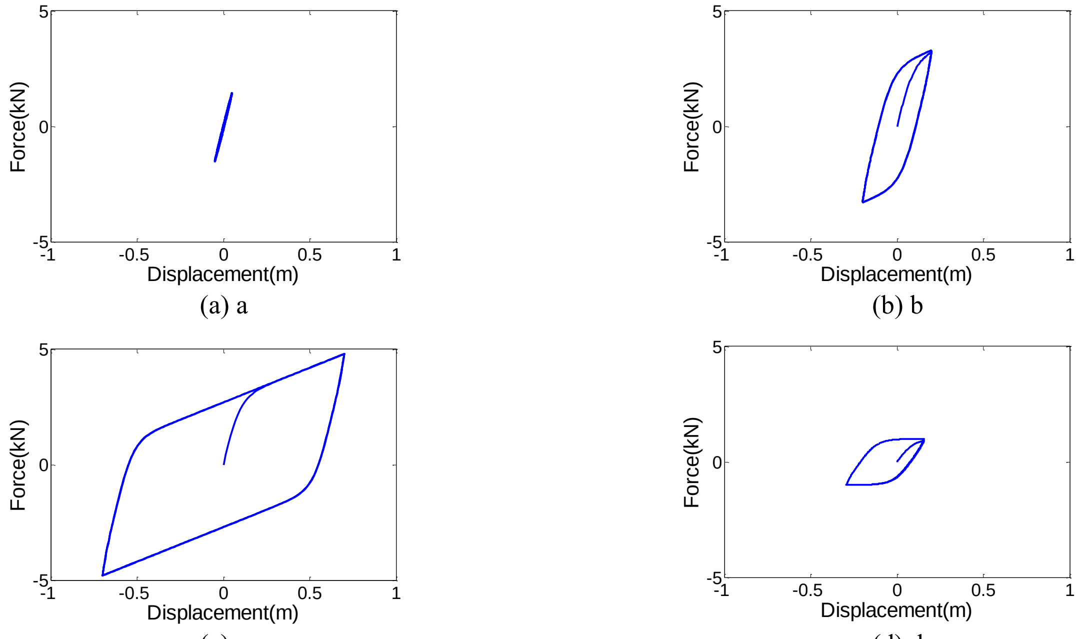

Fig. 2 Hysteretic loops for Scenarios a-d.

Table 4 Identified results of nonlinear hysteretic parameters of Case 1

Algorithms		u_y (m)	F_y (kN)	a (-)	γ (-)	n (-)
IEBL	Mean value	**0.1000**	**3.0000**	**0.1000**	**0.9000**	**2.0000**
	Relative error	0.00%	0.00%	0.00%	0.00%	0.00%
EBL	Mean value	0.1000	3.0003	0.1000	0.9009	1.9996
	Relative error	0.03%	0.01%	0.05%	0.10%	0.02%
CMFOA	Mean value	0.1396	4.0252	0.0632	0.9809	1.4559
	Relative error	39.65%	34.17%	36.80%	8.99%	27.21%
SSA	Mean value	0.1003	2.9999	0.1005	0.9189	2.0176
	Relative error	0.29%	0.00%	0.50%	2.10%	0.88%
Jaya	Mean value	0.1000	3.0001	0.1000	0.8999	2.0004
	Relative error	0.01%	0.00%	0.02%	0.01%	0.02%

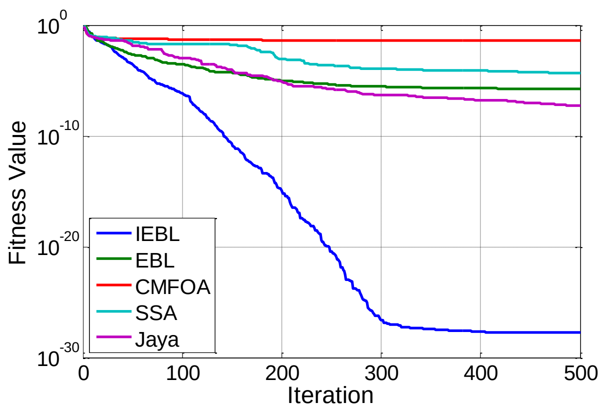

Fig. 3 Average evolutionary process for fitness value of Case 1

contain any information in the post-elastic state, as shown in Fig. 2(a). By contrast, the hysteretic parameters can be perfectly identified in Scenarios b-d without any error, in which strongly nonlinear hysteresis responses appear, as shown in Fig. 2(b)-(d). The average evolution processes of fitness values for the four scenarios are shown in Fig. 5. It can be observed that under loading Scenarios b-d, the identification needs about 320 iterations to converge while the performance obtained under loading Scenario a suffers a slow convergence problem after a few iterations. It can be inferred that the sensitivity of excitation input for nonlinear hysteresis parameter identification is weak if the to-be-identified system enters the post-elastic state.

4.2.3 Case 3: Identification of Scenario c with noise

This case study is to further investigate the sensitivity of the five algorithms to noise. Only the loading Scenario c is considered, i.e. a displacement-controlled sinusoidal loading $u = 7u_y \sin t$ with 10% uniform noise added to the response. Table 6 presents the final results of the identification of the five algorithms. It can be observed that IEBL, EBL, SSA, and Jaya are insensitive to measurement noise and yield promising estimation results with only small

Table 5 Identified results of nonlinear hysteretic parameters of Case 2.

Scenario		u_y (m)	F_y (kN)	a (-)	γ (-)	n (-)
a	Mean value	0.1190	3.5646	0.1514	0.9420	1.7793
	Relative error	19.01%	18.82%	51.39%	4.67%	11.03%
b	Mean value	0.1000	3.0000	0.1000	0.9000	2.0000
	Relative error	0.00%	0.00%	0.00%	0.00%	0.00%
c	Mean value	0.1000	3.0000	0.1000	0.9000	2.0000
	Relative error	0.00%	0.00%	0.00%	0.00%	0.00%
d	Mean value	0.1000	3.0000	0.1000	0.9000	2.0000
	Relative error	0.00%	0.00%	0.00%	0.00%	0.00%

Table 6 Identified results of nonlinear hysteretic parameters of Case 3

Algorithms		u_y (m)	F_y (kN)	a (-)	γ (-)	n (-)
IEBL	Mean value	**0.0999**	**3.0057**	**0.1003**	**0.9202**	**2.0062**
	Relative error	0.09%	0.19%	0.25%	2.24%	0.31%
EBL	Mean value	**0.0999**	**3.0057**	**0.1003**	**0.9202**	**2.0062**
	Relative error	0.09%	0.19%	0.25%	2.24%	0.31%
CMFOA	Mean value	0.1074	3.1521	0.0948	0.8886	1.7572
	Relative error	7.38%	5.07%	5.20%	1.27%	12.14%
SSA	Mean value	0.0991	3.0040	0.0994	0.8945	1.9551
	Relative error	0.93%	0.13%	0.63%	0.61%	2.24%
Jaya	Mean value	**0.0999**	**3.0057**	**0.1003**	**0.9202**	**2.0062**
	Relative error	0.09%	0.19%	0.25%	2.24%	0.31%

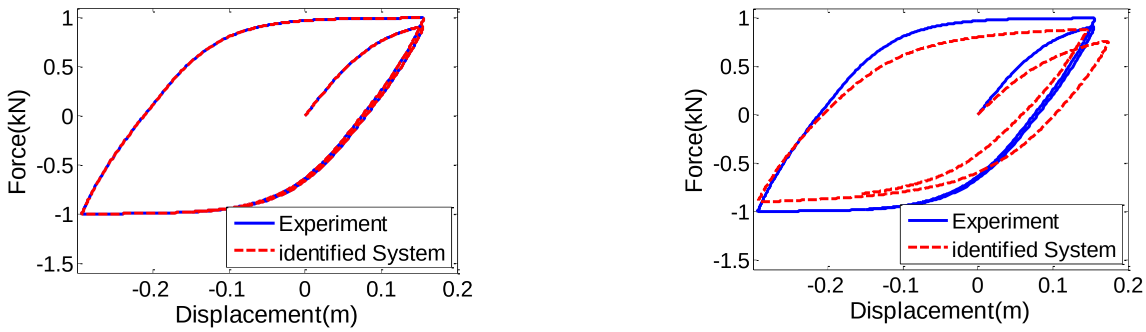

(a) IEBL (b) CMFOA

Fig. 4 Hysteretic loops obtained by IEBL and CMFOA of Case 1

relative errors ranging from 0.09% to 2.24%. As for CMFOA, it has unsatisfied performance in this case with a maximum estimation error of 12.14%. The average evolution processes of fitness values are shown in Fig. 6. It can be found that IEBL, EBL, SSA, and Jaya algorithms can converge to the minimum fitness value, among which IEBL has the fastest convergence speed and only needs around 50 iterations. This confirms the excellent computational efficiency of IEBL.

4.3 Parameter identification with viscous damping

The above case studies demonstrate that accurate identification results can be achieved by using IEBL for the SDOF system with no viscous damping in the hysteresis Bouc-Wen model. To further assess the performance of the proposed IEBL, the SDOF hysteretic system with viscous damping is considered in this section and unknown

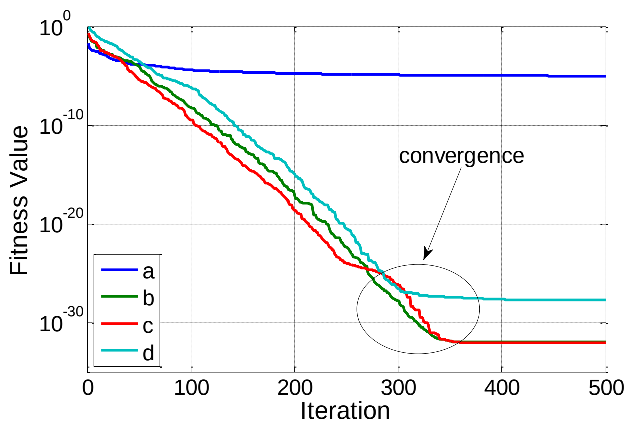

Fig. 5 Average evolutionary process for fitness value of Case 2

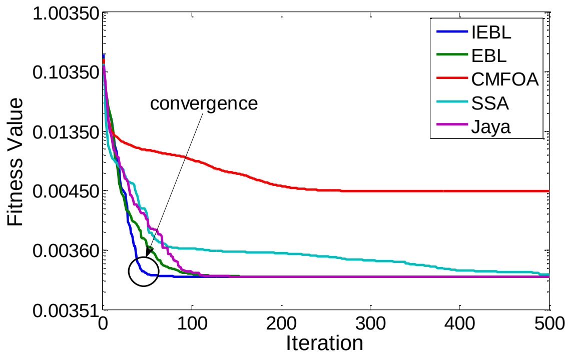

Fig. 6 Average evolutionary process for fitness value of Case 3

Table 7 True values and lower and upper bound constraints in the cases with viscous damping

Parameters	u_y (m)	F_y (kN)	α (-)	γ (-)	n (-)	c (kNs/m)
True values	0.1	3	0.1	0.9	2	5
Lower bound	0	0	0	0	0	0
Upper bound	1	10	1	1	10	100

parameters thus become six, that is u_y, F_y, α, γ, n, and c. Scenarios b-d are considered in order to ensure that the system enters the post-elastic state. The true parameter values and the lower and upper bound constraints are listed in Table 7. The other settings are the same as those in Section 4.2.

4.3.1 Case 4: Identification of Scenarios d without noise

This case study aims to investigate the performance of IEBL for the identification of hysteretic parameters of Bouc-Wen nonlinear model with viscous damping by comparing with EBL, CMFOA, SSA, and Jaya. The identification results are exhibited in Table 8. It can be observed that exactly accurate parameter values up to four decimal digits can be obtained by IEBL, and the maximum errors of EBL and Jaya are acceptable and equal 0.09% and 3.05%, respectively. Even though this case has no noise corruption, CMFOA and SSA yet completely failed to identify the assumed values with maximum errors as large as 142.86% and 128.68%, respectively. It should bear in mind that the maximum relative errors obtained by CMFOA and SSA in Case 1 (Section 4.2.1) are 39.65% and 2.10%, respectively. This reveals that it is more difficult to identify the nonlinear parameter accurately of a system with viscous damping than that without damping. Fig. 7 shows the average evolution process of the logarithmic fitness values in ten independent runs. It is obvious that IEBL achieves a very small error at a magnitude of 10^{-28} with a much faster convergence speed than the other algorithms, which indicates an excellent identification performance of the proposed method. In contrast, EBL, CMFOA, SSA, and Jaya may be stuck to local optima and thus easily cease convergence with unsatisfactory identified results. Once again, the superiority of the proposed IEBL has demonstrated for its identification accuracy of nonlinear hysteretic parameters.

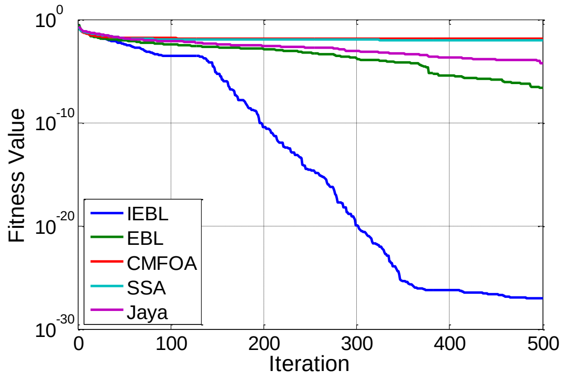

Fig. 7 Average evolutionary process for fitness value of Case 4

4.3.2 Case 5: Influence of excitation input with viscous damping

Different excitation inputs are considered to examine their influence on the performance of IEBL and the original EBL. Table 9 lists a summary of the identified results of Scenarios b-d. It can be found that the proposed IEBL accurately identify the nonlinear hysteresis parameters without any estimation error in all scenarios, which demonstrates again that the proposed method is insensitive to excitation input. These identification results of IEBL are better than those of the original EBL. As per Table 9, EBL seems to obtain better and better identification results from Scenario b to Scenario d with the maximum error decreasing from 3.84% to 0.09%. That is to say, the original EBL is still a bit sensitive to excitation input. Fig. 8 shows the average evolution processes of fitness values for the three scenarios in a logarithmic form, in which IEBL reaches a small fitness value in an order of 10^{-28} while EBL can only achieve an order of 10^{-8}. This also validates that the convergence performance of the proposed IEBL is significantly improved.

4.3.3 Case 6: Influence of noise level

The objective of this study is to examine the effect of noise level on nonlinear parameter identification performance of the IEBL. Two noise levels (5% and 10%) are added into the original time history of acceleration in Scenario d and the final identified results are presented in Table 10. It is found that the proposed IEBL can achieve a small maximum error of 1.23% under the noise level of 5%. The identified results are still acceptable with a fair level of accuracy even under the noise levels of 10%. Taken the identified nonlinear parameter γ as an example (Fig. 9), the proposed IEBL converges to the preset true value 0.9 at around 150-th iteration and after that the evolutionary curves are quite stable. Although the relative error of the identified parameter γ increases gradually with the increase of noise level, the maximum error is still small even with as high as 10% noise level. Fig. 10 shows the true acceleration and the calculated acceleration with the identified parameters under 10% noise level condition. A very good match can be achieved between these two curves. This indicates the superiority of using IEBL for nonlinear system identification and also reveals that the proposed method is insensitive to measurement noise.

Table 8 Identified results of nonlinear hysteretic parameters of Case study 4

Algorithms		u_y (m)	F_y (kN)	a (-)	γ (-)	n (-)	c (kNs/m)
IEBL	Mean value	**0.1000**	**3.0000**	**0.1000**	**0.9000**	**2.0000**	**5.0000**
	Relative error	0.00%	0.00%	0.00%	0.00%	0.00%	0.00%
EBL	Mean value	0.1000	2.9997	0.1001	**0.9000**	2.0004	5.0005
	Relative error	0.01%	0.01%	0.09%	0.00%	0.02%	0.01%
CMFOA	Mean value	0.2429	7.1540	0.0304	0.4782	0.6748	9.9136
	Relative error	142.86%	138.47%	69.55%	46.87%	66.26%	98.27%
SSA	Mean value	0.1997	6.8605	0.0176	0.4378	0.7197	8.8175
	Relative error	99.72%	128.68%	82.36%	51.36%	64.01%	76.35%
Jaya	Mean value	0.1002	2.9991	0.1030	0.8967	2.0030	5.0485
	Relative error	0.20%	0.03%	3.05%	0.37%	0.15%	0.97

Table 9 Identified results of nonlinear hysteretic parameters of Case 5

Algorithm	Scenario		u_y (m)	F_y (kN)	a (-)	γ (-)	n (-)	c (kNs/m)
IEBL	b	Mean value	0.1000	3.0000	0.1000	0.9000	2.0000	5.0000
		Relative error	0.00%	0.00%	0.00%	0.00%	0.00%	0.00%
	c	Mean value	0.1000	3.0000	0.1000	0.9000	2.0000	5.0000
		Relative error	0.00%	0.00%	0.00%	0.00%	0.00%	0.00%
	d	Mean value	0.1000	3.0000	0.1000	0.9000	2.0000	5.0000
		Relative error	0.00%	0.00%	0.00%	0.00%	0.00%	0.00%
EBL	b	Mean value	0.1000	2.9988	0.1003	0.9001	2.0011	5.1920
		Relative error	0.03%	0.04%	0.33%	0.01%	0.05%	3.84%
	c	Mean value	0.1001	3.0013	0.1000	0.9019	2.0005	4.9377
		Relative error	0.08%	0.04%	0.01%	0.21%	0.02%	1.25%
	d	Mean value	0.1000	2.9997	0.1001	0.9000	2.0004	5.0005
		Relative error	0.01%	0.01%	0.09%	0.00%	0.02%	0.01%

Table 10 Identified results of nonlinear hysteretic parameters of Case 6

Noise level		u_y (m)	F_y (kN)	a (-)	γ (-)	n (-)	c (kNs/m)
0	Mean value	0.1000	3.0000	0.1000	0.9000	2.0000	5.0000
	Relative error	0.00%	0.00%	0.00%	0.00%	0.00%	0.00%
5%	Mean value	0.0999	2.9974	0.1012	0.9097	2.0095	4.9490
	Relative error	0.06%	0.09%	1.23%	1.08%	0.48%	1.02%
10%	Mean value	0.0998	2.9884	0.1041	0.9327	2.0466	4.8453
	Relative error	0.24%	0.39%	4.13%	3.63%	2.33%	3.09%

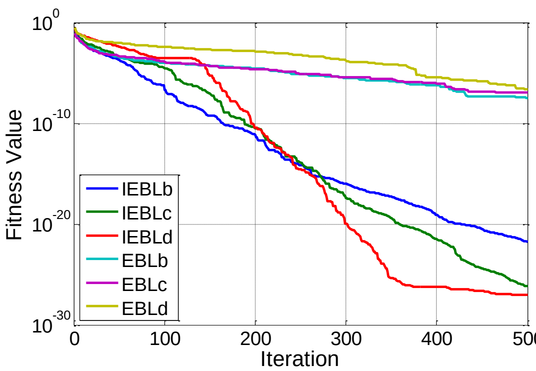

Fig. 8 Average evolutionary process for fitness value of Case 5

5. Laboratory test of lead-filled steel tube dampers and their parameter identification

5.1 Cyclic loading test of lead-filled steel tube dampers

In this section, a set of experimental data from Zhou *et al*. (2017) is utilized to identify hysteretic parameters of a lead-filled steel tube damper (LFSTD) to verify the superiority of the proposed IEBL algorithm. The LFSTD consists of a steel tube, a lead cylinder, and two steel plate caps, as shown in Fig. 11. The steel tube is made of a seamless steel tube with a category of #20 in Chinese standard, the exterior surface of which is profiled in a

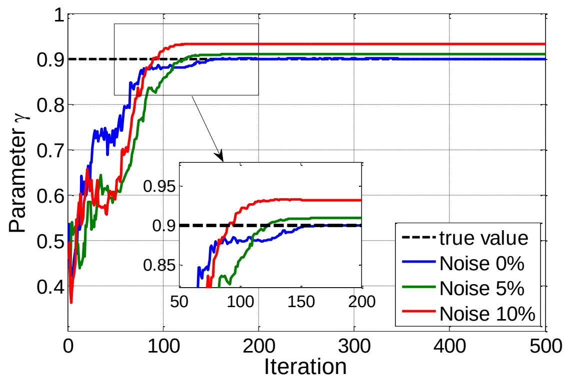

Fig. 9 Average evolution process for parameter γ of Case 6

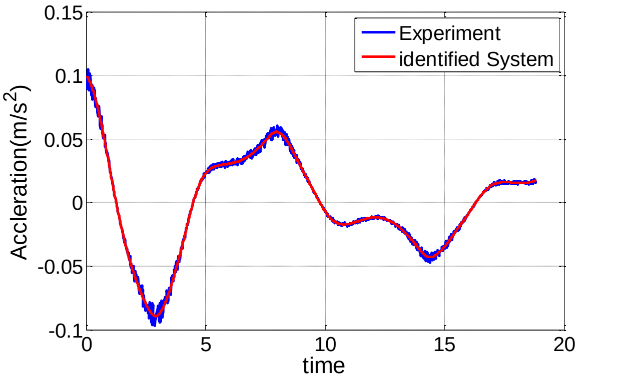

Fig. 10 True and calculated acceleration responses with 10% noise of Case 6

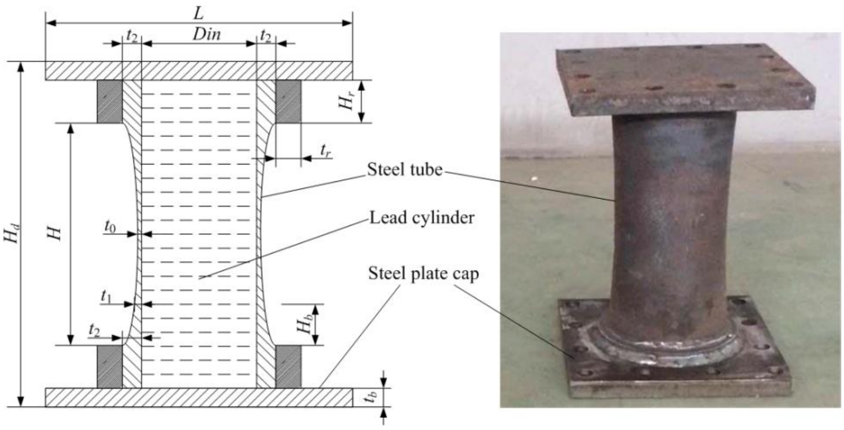

Fig. 11 Geometry of LFSTD

Table 11 Structural parameters of test specimens (Unit: mm)

Specimen No.	H_d	H	Din	t_2	t_1	t_0	H_b	H_r×t_r	L×t_b
LFSTD-1	400	300	150	11	6	3	20	25×20	270×25
LFSTD-2	400	300	150	14	8	4	20	25×20	270×25
LFSTD-3	400	300	150	17	10	5	20	25×20	270×25
LFSTD-4	400	300	150	14	8	3.2	20	25×20	270×25
LFSTD-5	400	300	150	14	8	4.8	20	25×20	270×25
LFSTD-6	450	350	150	14.33	8	4	23.3	25×20	270×25
LFSTD-7	500	400	150	14.67	8	4	26.7	25×20	270×25

parabolic shape in order to ensure that the deformation and energy dissipation of the LFSTD mainly occur in its middle section. The lead cylinder (Pb99.990) is commonly adopted in the design of passive earthquake-resistant dampers because of its promising plastic deformation ability and energy absorption ability. The two caps are made of Q235 steel and are corrected with a targeted seismic-resistant structure by blots. The LFSTD has the following merits: (a) both steel and lead are stable and durable materials and their combination has a promising energy absorption ability, (b) the lead cylinder causes no pollution because it is placed inside the steel tube and does not need to be welded, (c) its structure is simple and convenient to manufacture with low cost, and (d) it is easy to install and replace.

Table 12 Lower and upper bound constraints of the experimental model.

Parameters	u_y (m)	F_y (kN)	α (-)	γ (-)	n (-)	c (kNs/m)
Lower bound	0	0	0	0	0	0
Upper bound	5	500	1	1	10	100

Table 11 lists the design dimension of seven LFSTDs manufactured at Guangzhou University, China (Zhou *et al.* 2017). A cyclic loading test was carried out on these seven LFSTDs in a platform shown in Fig. 12, in which two vertical steel frames are hinged in order to ensure horizontal movement of the test specimen. In the test, a hydraulic actuator cyclically pushes the top steel frame of the

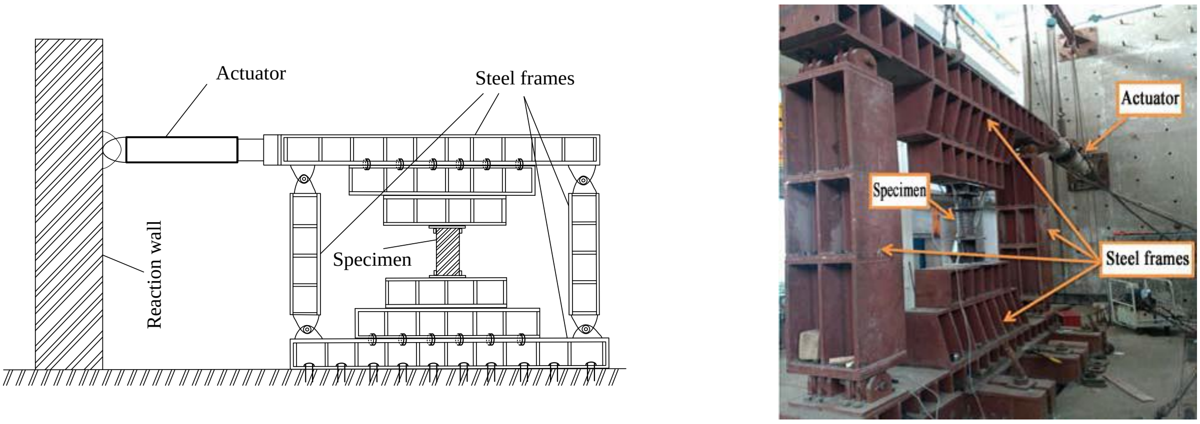

(a) Sketch (b) Picture

Fig. 12

Table 13 Final identified parameter values using IEBL

Specimen No.		u_y (m)	F_y (kN)	α (-)	γ (-)	n (-)	c (kNs/m)
LFSTD-1	Mean value	0.9121	271.7108	0.0083	0.4198	0.1588	5.2025
	Best value	0.7762	272.4978	0.0068	0.3414	0.1291	5.1109
LFSTD-2	Mean value	0.9013	361.4261	0.0073	0.5239	0.1528	4.1653
	Best value	0.6994	361.1877	0.0056	0.3958	0.1127	4.7956
LFSTD-3	Mean value	0.5401	437.6155	0.0027	0.1875	0.1003	14.8495
	Best value	0.3529	442.0305	0.0016	0.1203	0.0599	13.3095
LFSTD-4	Mean value	0.5233	285.0112	0.0066	0.3019	0.1341	20.7546
	Best value	0.4129	281.3155	0.0054	0.2337	0.1091	22.1413
LFSTD-5	Mean value	0.7171	389.1734	0.0059	0.2649	0.1145	28.6998
	Best value	0.3897	400.0357	0.0026	0.1312	0.0540	25.7215
LFSTD-6	Mean value	0.6284	309.8575	0.0047	0.2479	0.1694	18.3896
	Best value	0.5184	307.1141	0.0040	0.1992	0.1432	19.2226
LFSTD-7	Mean value	0.8345	290.1381	0.0044	0.2756	0.1956	11.2239
	Best value	0.7838	291.0453	0.0040	0.2568	0.1771	11.1229

platform and then causes a cyclic motion of the LFSTD. A displacement-controlled loading strategy is adopted, and the loading started from 0.3 mm to 30 mm in 10 steps and each step is repeated for three cycles. The loading frequency is 0.02 Hz. The force of the actuator is collected by its force sensor, and the displacement of the LFSTD is measured by a displacement transducer.

5.2 Identified results

Nonlinear hysteretic parameters of the Bouc-Wen model for the seven LFSTDs are identified using IEBL, the original EBL, and the other four algorithms based on the measured displacement-force data. The settings of these algorithms are the same as the numerical studies in Section 4. The lower and upper bound constraints of identified parameters are summarized in Table 12, in which the constraints of parameters u_y and F_y are chosen from a simple inspection of the experimental force-displacement diagram. For each LFSTD, ten independent runs are taken and the best solution of each algorithm is kept and compared.

Fig. 13 presents the evolution of the best run of each algorithm for all seven LFSTDs in a logarithmic form, which is used as an indicator to examine the algorithm performance. In terms of the best run performance, it is found that IEBL manages to outperform the other four algorithms especially at the later iterations, which further demonstrates the excellent robustness of the proposed IEBL. Table 13 lists the final identification results of all LFSTDs using IEBL, including the mean parameter values of ten runs and the values of the best run. Fig. 14 compares the experimental displacement-force loops with the hysteresis loops of the identified system obtained by the best run of IEBL. It can be observed that the loops of the identified system are in very good agreement with the experimental ones for all LFSTDs. The final values of normalized MSE are very small, which are 0.71%, 1.13%, 1.87%, 1.43%, 1.09%, 2.61%, and 2.97% for LFSTDs 1-7, respectively. These small MSE values also serve as another index to confirm the excellent performance of IEBL in identifying nonlinear hysteretic parameters that govern the hysteretic response. From an engineering point of view, it can be stated that the identification results of the IEBL are adequate for nonlinear hysteretic parameter analysis.

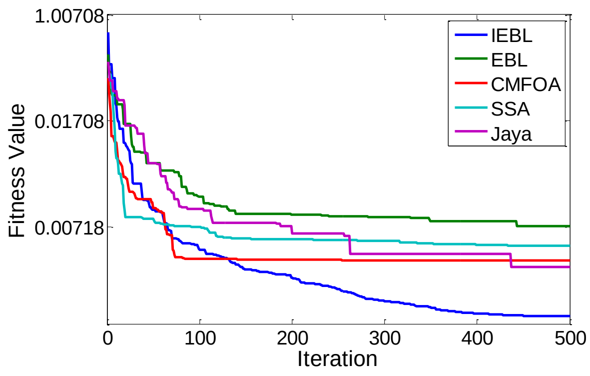

(a) LFSTD-1

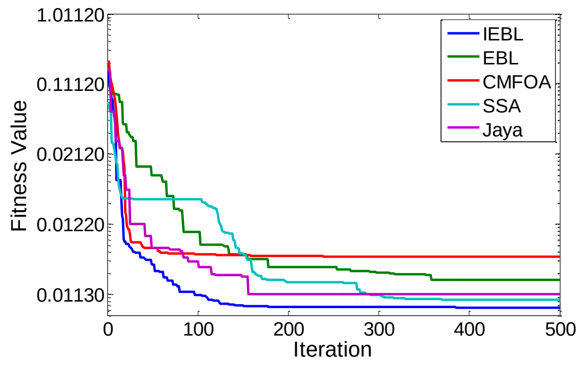

(b) LFSTD-2

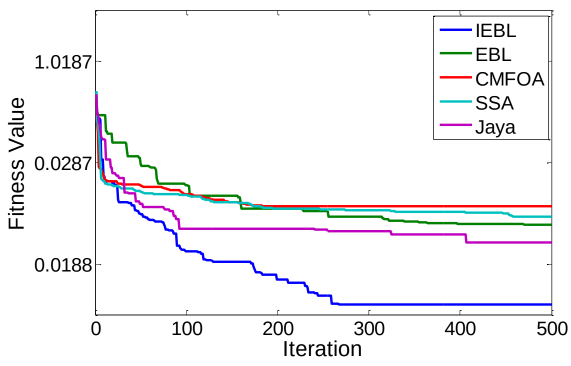

(c) LFSTD-3

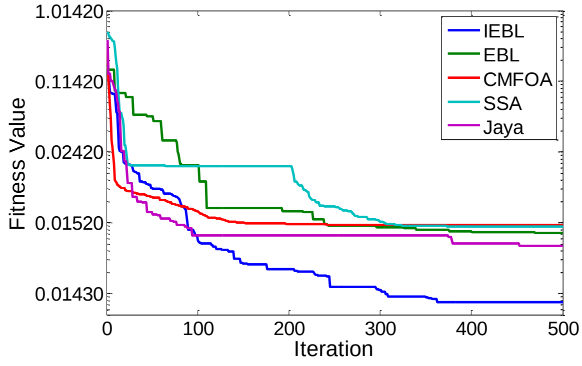

(d) LFSTD-4

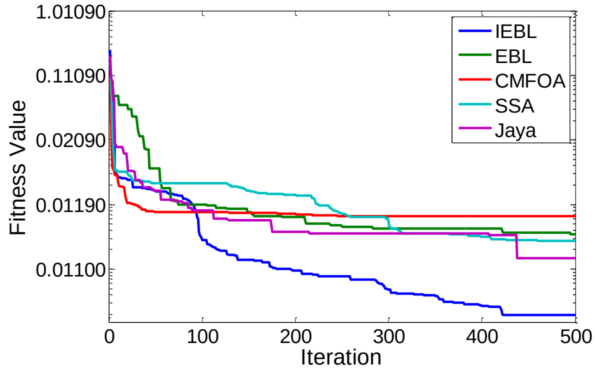

(e) LFSTD-5

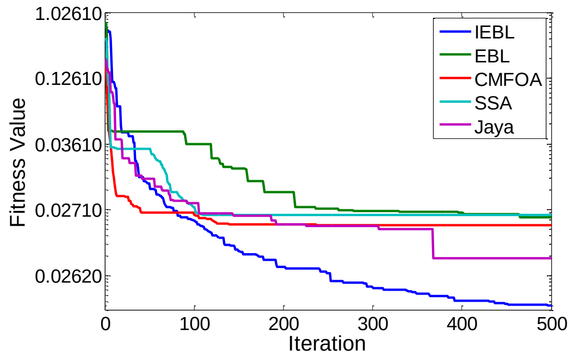

(f) LFSTD-6

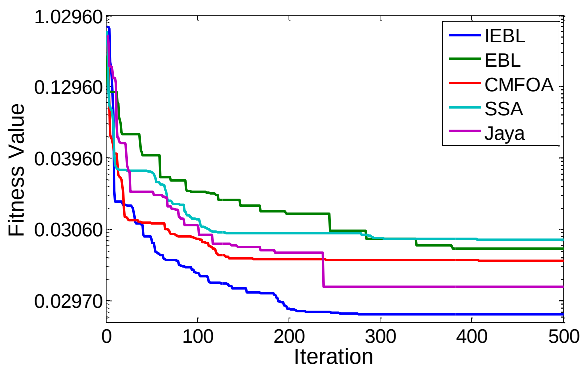

(g) LFSTD-7

Fig. 13 Evolutionary process for fitness value of the best run of each algorithm

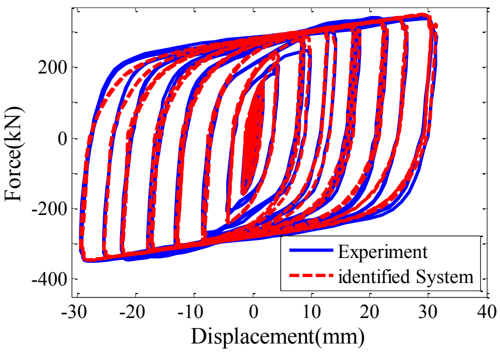

(a) LFSTD-1

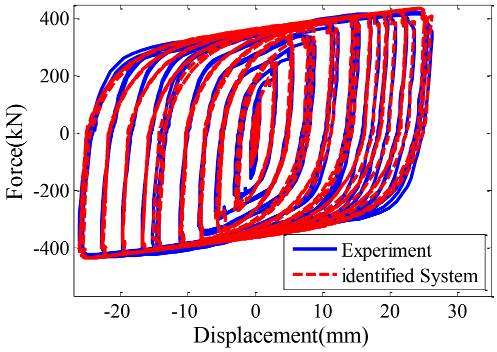

(b) LFSTD-2

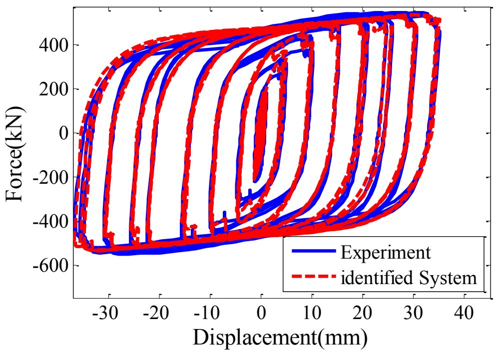

(c) LFSTD-3

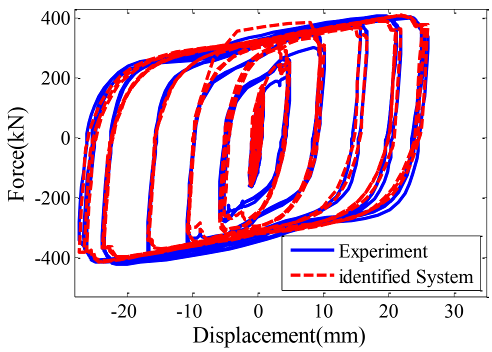

(d) LFSTD-4

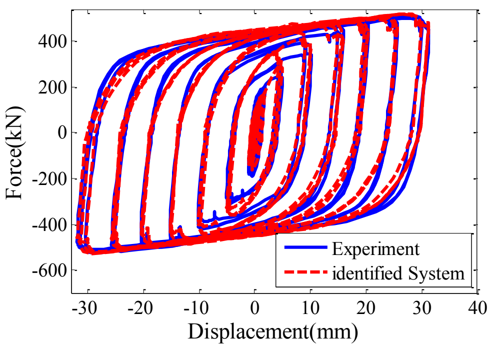

(e) LFSTD-5

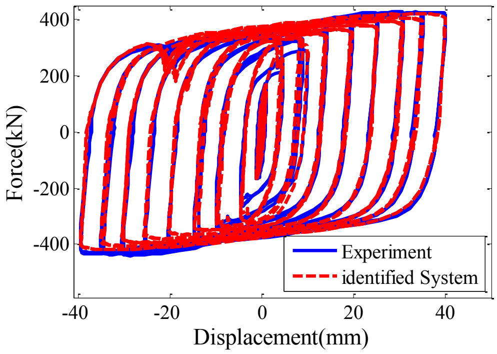

(f) LFSTD-6

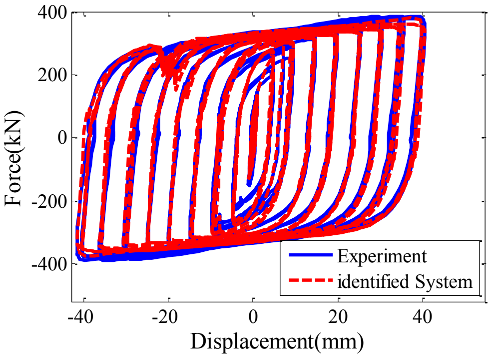

(g) LFSTD-7

Fig. 14 The experimental and identified hysteretic loops.

6. Conclusions

In this paper, an improved experience-based learning algorithm is presented for nonlinear parameter identification of Bouc–Wen hysteretic system. Two modifications, including the quasi-oppositional learning and the new updating equations, are incorporated to modify the original EBL for improvement of global optimization ability. The efficiency and robustness of the proposed algorithm are investigated by parameter identification of a nonlinear SDOF system with hysteresis Bouc-Wen model and of seven lead-filled steel tube dampers. Through these investigations, several conclusions can be drawn as follows:

- The effectiveness of the IEBL is insensitive to excitation input if the system enters the post-elastic state.
- Numerical results show that the IEBL is insensitive to noise and is able to identify both the hysteretic parameter as well as viscous damping with small relative errors (less than 4.13%).
- Laboratory test results of seven lead-filled steel tube dampers confirm the efficiency of the IEBL in nonlinear identification of Bouc–Wen hysteretic parameters for practical application and the normalized mean square error values range from 0.71% to 2.97%.
- Both numerical and experimental studies demonstrate that the IEBL manages to obtain better identification performance compared with the other four algorithms (EBL, CMFOA, SSA, and Jaya).

Acknowledgments

This work is supported by a research grant from the National Natural Science Foundation of China (51808147).

References

Artar, M. and Daloglu, A.T. (2019), "Optimum design of steel space truss towers under seismic effect using Jaya algorithm", *Struct. Eng. Mech.*, **71**(6), 1-12. http://dx.doi.org/10.12989/sem.2019.71.1.001.

Bajrić, A. and Høgsberg, J. (2018), "Estimation of hysteretic damping of structures by stochastic subspace identification", *Mech. Syst. Signal Proc.*, **105**, 36-50. http://dx.doi.org/10.1016/j.ymssp.2017.11.042.

Chang, C.C. and Shi, Y. (2010), "Identification of time-varying hysteretic structures using wavelet multiresolution analysis", *Int. J. Non-Linear Mech.*, **45**(1), 21-34. http://dx.doi.org/10.1016/j.ijnonlinmec.2009.08.009.

Ding, Z., Li, J., Hao, H. and Lu, Z.R. (2019), "Nonlinear hysteretic parameter identification using an improved tree-seed algorithm", *Swarm Evol. Comput.*, **46**, 69-83. http://dx.doi.org/10.1016/j.swevo.2019.02.005.

Dong, H., Han, Q. and Du, X. (2019), "Application of an extended Bouc-Wen model for hysteretic behavior of the RC structure with SCEBs", *Struct. Eng. Mech.*, **71**(6), 683-697. http://dx.doi.org/10.12989/sem.2019.71.6.683.

Jain, M., Singh, V. and Rani, A. (2019) "A novel nature-inspired algorithm for optimization: Squirrel search algorithm", *Swarm Evol. Comput.*, **44**, 148-175. http://dx.doi.org/10.1016/j.swevo.2018.02.013.

Korayem M.H. and Homayouni, A. (2017) "The size-dependent analysis of multilayer micro-cantilever plate with piezoelectric layer incorporated voltage effect based on a modified couple stress theory", *Eur. J. Mech. A-Solids*, **61**, 59-72. http://dx.doi.org/10.1016/j.euromechsol.2016.08.013.

Korayem, M.H. and Sadeghzadeh, S. (2009) "A new modeling and compensation approach for creep and hysteretic loops in SPM's piezotubes", *Int. J. Adv. Manuf. Technol.*, **44**(7-8), 1133-1143. http://dx.doi.org/10.1007/s00170-009-1926-x.

Korayem M.H., Sadeghzadeh, S. and Rahneshin, V. (2012) "A new multiscale methodology for modeling of single and multi-body solid structures", *Comput. Mater. Sci.*, **63**, 1–11. http://dx.doi.org/10.1016/j.commatsci.2012.05.059.

Li, Z. and Shu, G. (2019), "Hysteresis characterization and identification of the normalized Bouc-Wen model", *Struct. Eng. Mech.*, **70**(2), 209-219. http://dx.doi.org/10.12989/sem.2019.70.2.209.

Ma, F., Zhang, H., Bockstedte, A., Foliente, G.C. and Paevere, P. (2004), "Parameter analysis of the differential model of hysteresis", *J. Appl. Mech.*, **71**, 342-9. http://dx.doi.org/10.1007/978-94-010-0179-3_22.

Mahdavi, S., Rahnamayan, S. and Deb, K. (2018), "Opposition based learning: A literature review", *Swarm Evol. Comput.*, **39**, 1-23. http://dx.doi.org/10.1016/j.swevo.2017.09.010.

Niola, V., Palli, G., Strano, S. and Terzo, M. (2019), "Nonlinear estimation of the Bouc-Wen model with parameter boundaries: Application to seismic isolators", *Comput. Struct.*, **222**, 1-9. http://dx.doi.org/10.1016/j.compstruc.2019.06.006.

Omrani, R., Hudson, R.E. and Taciroglu, E. (2012), "Parametric identification of nondegrading hysteresis in a laterally and torsionally coupled building using an unscented Kalman filter", *J. Eng. Mech.*, **139**(4), 452-468. http://dx.doi.org/10.1061/(ASCE)EM.1943-7889.0000498.

Ortiz, G.A., Alvare,z D.A., Bedoya-Ruíz, D. (2013), "Identification of Bouc-Wen type models using multi-objective optimization algorithms", *Comput. Struct.* **114-115**, 121-132. http://dx.doi.org/10.1016/j.compstruc.2012.10.016

Quaranta, G., Marano, G.C., Greco, R. and Monti, G. (2014), "Parametric identification of seismic isolators using differential evolution and particle swarm optimization", *Appl. Soft. Comput.*, **22**, 458-464. http://dx.doi.org/10.1016/j.asoc.2014.04.039.

Shu, G. and Li, Z. (2017), "Parametric identification of the Bouc-Wen model by a modified genetic algorithm: Application to evaluation of metallic dampers", *Earthq. Struct.*, **13**(4), 397-407.

Tran, C.T.N. and Li, B. (2018), "Seismic performance of RC short columns with light transverse reinforcement", *Struct. Eng. Mech.*, **67**(1), 93-104. http://dx.doi.org/10.12989/sem.2018.67.1.093.

Worden, K. and Manson, G. (2012), "On the identification of hysteretic systems. Part I: Fitness landscapes and evolutionary identification", *Mech. Syst. Signal Proc.*, **29**, 201-212. http://dx.doi.org/10.1016/j.ymssp.2012.01.004.

Zheng, T., Liu, J., Luo, W. and Lu, Z. (2018), "Structural damage identification using cloud model based fruit fly optimization algorithm", *Struct. Eng. Mech.*, **67**(3), 245-254. http://dx.doi.org/10.12989/sem.2018.67.3.245.

Zheng, T., Luo, W., Hou, R., Lu, Z. and Cui, J. (2019), "A novel experience-based learning algorithm for structural damage identification: simulation and experimental verification", *Eng. Optimiz.*, 1-24. http://dx.doi.org/10.1080/0305215X.2019.1668935.

Zhou, Y., Lu, D. and Zhang, M. (2017), "Study on mechanical properties of lead-filled steel tube damper", *China Civ. Eng. J.*, **50**(1), 46-52. (in Chinese)

CC